

# LATEST LATTICE DESIGN AND OPTIMIZATION FOR THE SOUTHERN ADVANCED PHOTON SOURCE STORAGE RING

Yu Zhao, Yi Jiao\*, Weihang Liu, Jianliang Chen, Xiao Li, Xingguang Liu, Sheng Wang<sup>†</sup>

Institute of High Energy Physics, Beijing, China

also at Spallation Neutron Source Science Center, Dongguan, Guangdong, China

## Abstract

The Southern Advanced Photon Source (SAPS) is a 3.5 GeV, kilometer-scale, ultra-low emittance storage ring to be built next to the China Spallation Neutron Source in Guangdong Dongguan, China. A preliminary lattice design for SAPS storage ring with an emittance of 31.8 pm·rad has been proposed before. Now, the SAPS lattice is continuously under extensive design and optimization. In this paper, the latest design of lattice is introduced, and the linear and nonlinear performance is presented.

## INTRODUCTION

Pursuing for higher brightness and better coherence of X-ray has been the main motivation for the development of storage ring light sources. A particularly effective way to achieve high radiation brightness is to reduce the electron beam emittance. In the past years, with the continuous advance in accelerator technology [1–3] and extensive studies made to explore unit cells to minimize the emittance (for example, a unit cell, which is proposed by SLS 2.0 [4], consists of a longitudinal gradient bend (LGB) [5] and reverse bends (RBs) [6], allows the emittance to reach or below the theoretical minimum emittance), the emittance has been pushed down to hundreds or even tens of pm·rad, which is nearly or approach the diffraction limit of X-rays. Such ultra-low emittance storage rings are usually called diffraction-limited storage rings (DLSRs), which are regarded as the fourth generation light sources [7]. Nowadays, Many facilities, including MAX-IV [8], Sirius [9], ESRF-EBS [10], APS-U [11], HEPS [12], HLAf [13], and many others are under design, construction, commissioning or operation. As one of these facilities, the Southern Advanced Photon Source (SAPS), is a mid-energy ultra-low emittance ring-based light source proposed to be built adjacent to the China Spallation Neutron Source.

Due to the capability of the hybrid-MBA (H-MBA) lattice to simultaneously realize excellent nonlinear performance and ultra-low emittance, a preliminary design [14, 15] (named Design I) has been designed for the SAPS based on modified H-MBAs where one LGB/RB and two TLGB/RB unit cells (the LGB in the LGB/RB unit cell could be simplified by a bend combined with horizontal and longitudinal gradients (TLGB) to compose a TLGB/RB unit cell) are adopted therein to control the damping time to a reasonable level. The design provides a beam with the energy of 3.5 GeV and a current of 200 mA. Besides, with 36 periods of

H-7BAs and a circumference of 1080 m, an emittance of 31.8 pm·rad is obtained. The horizontal and vertical DAs are 4 mm, and the MA is 3%, which meet the requirements of on-axis swap-out injection.

Now, the SAPS lattice is continuously undergoing extensive design and optimization, and the requirements for SAPS are gradually being clarified as follows,

- (1) the natural emittance should be lower than 60 pm·rad;
- (2) the circumference should be smaller than 1000 m;
- (3) the long straight section (LSS) is fixed at 6 m to allow sufficient space to accommodate insertion devices (IDs);
- (4) the damping time should be smaller than 30 ms;
- (5) the nonlinear dynamics performance should be large enough to meet the requirements of on-axis swap-out injection and candidate longitudinal injection;
- (6) a larger beam current is pursued to further improve the photon flux and to achieve higher brightness up to  $1 \times 10^{22}$  ph/s/mrad<sup>2</sup>/mm<sup>2</sup>/0.1%BW at a photon energy of about 4 keV.

Based on the above, a new lattice has been designed for SAPS.

## LINEAR OPTICS

Firstly, the lattice (named Design II) with a shorter circumference is considered. The periods are changed from 36 to 32 and the length of one period lattice is reduced from 30 m to 25.3 m, resulting in a circumference of 810 m (the harmonic number is 450 for 166.6 MHz RF cavities). In order to achieve such a compact layout, the three central cells of Design I are all replaced by TLGB/RB unit cells (named unit B), as shown in Fig. 1(b). Compared to the LGB/RB unit cell (named unit A) in Design I, unit B is found to allow a shorter cell length with a similar emittance under the SAPS parameters (the comparison result is shown in the Ref. [16]). The TLGB is divided into three slices. The central slice is a high field dipole with the length of 0.166 m, and the other two slices are dipoles combined with horizontally defocusing gradient (BDs) of below 25 T/m, which is limited by the current international production process of taper dipole design [17]. Similar to Design I, the maximum dipole fields of three TLGBs are still 1.3 T, 2 T and 1.3 T, respectively. The horizontal and vertical phase advances between each pair of sextupoles are matched to be  $3\pi$  (-I transformation) [18] and  $2\pi$  to eliminate most of the nonlinear effect caused by the sextupoles.

Then, a horizontally focusing quadrupole field (Q3) is added inside the outer LGBs (i.e. the first and the seventh bends in the modified H-7BA) to increase the dispersion

\* jiaoyi@ihep.ac.cn

<sup>†</sup> wanggs@ihep.ac.cn

functions along the outer LGBs, so as to increase the momentum compact factor. Besides above, the addition of Q3 helps focus the beta functions at the center of LSS for higher brightness. Meanwhile, the possibility of matching the optimum beta function ( $\beta_x = \beta_y = L/\pi$ ,  $\beta_x$  and  $\beta_y$  are beta functions at the center of the LSS,  $L$  is the length of the IDs) is preserved to yield the maximum brightness and to achieve horizontal and vertical full coupling via difference resonance [19, 20]. It is noticed that the magnets between the second and the sixth bends of the current scheme are all combined-function dipoles, which greatly limits the adjustability and flexibility of the design. Therefore, two horizontally defocusing quadrupoles (Q9) are added between the third and fourth dipoles, and between the fourth and the fifth dipoles, as shown in the Fig. 1(c). In addition, to find a balance between the emittance, momentum compact factor and damping time, the highest fields of the TLGBs are adjusted to 0.9 T, 2 T and 0.9 T, respectively. Moreover, the horizontal and vertical phase advances of one period lattice are matched close to be  $(39/16, 22/16) \times 2\pi$ , so that the first and second order nonlinear resonance driving terms generated by sextupoles could be minimized over 16 periods. The chromaticities are corrected to  $[+5, +5]$  with three families of sextupoles (SD1, SD2, and SF) to avoid collective instabilities.

Finally, the momentum compact factor is increased to  $3.61 \times 10^{-5}$  (Design III) with an emittance of 26.3 pm-rad and damping time of 25 ms. The optical functions of the Design III are shown in Fig. 2, and the parameters are shown in Table 1.

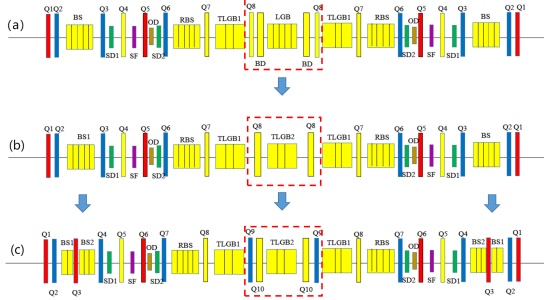


Figure 1: Layouts of Design I (a), Design II (b) and Design III (c) for SAPS. A red and blue box represent QF and QD, respectively; a yellow box represents bends; green and purple box represent SD and SF, respectively; brown box represents octupole (BS and RBS represent the LGBs).

## NONLINEAR DYNAMICS PERFORMANCE

At the present stage of nonlinear optimization, three pairs of sextupoles are regrouped as independent knobs to enlarge the DA and MA. Two chromatic sextupoles among 6 sextupole knobs are assigned for chromaticity correction and the rest 4 sextupoles accompany with 2 octupoles to enlarge DA and minimize tune-shifts with amplitude or momentum.

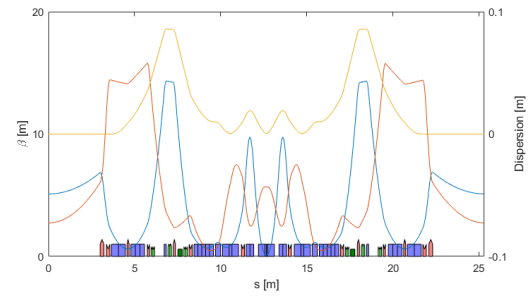


Figure 2: Optical functions of Design III for SAPS. Blue, red, green, and dark green blocks represent dipoles, quadrupoles, sextupoles and octupoles, respectively.

Figure 3 (a) shows the tune-shifts with momentum deviation of Design III, indicating that the MA is nearly 4%. To calculate the local MA, 6D particle tracking over 1024 turns is performed, considering that the frequency of the RF cavity is 166.6 MHz and its voltage is 2 MV. The result is shown in Fig. 3 (b). The minimum MA is nearly 4%.

The on-momentum DA at the middle of the LSS and its frequency map analysis are shown in Fig. 4, through particle tracking over 1024 turns. The horizontal and vertical DAs are larger than 5 mm.

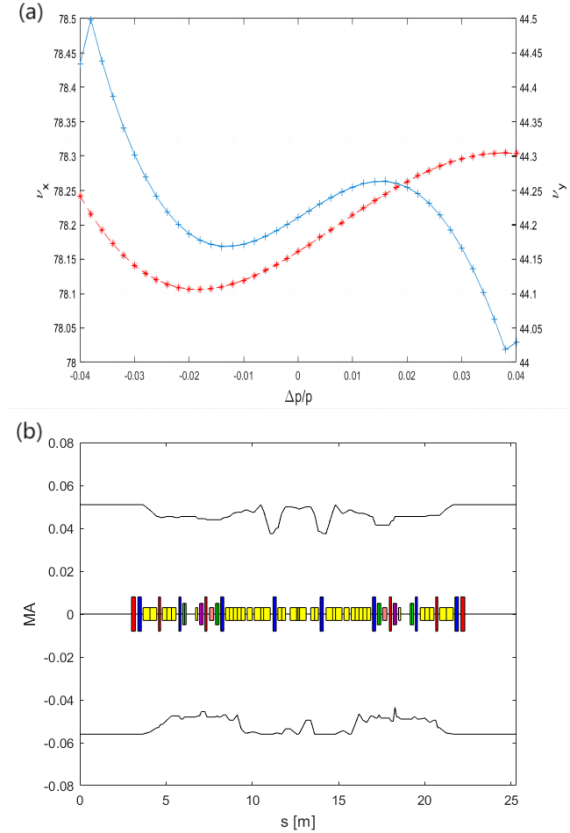


Figure 3: Tune-shifts with momentum deviation of Design III for SAPS (a) and local MA along one period of Design III for SAPS, tracked over 1024 turns with 6D tracking (b).

Table 1: Main Parameters of Three Lattices

Parameters	Design I	Design II	Design III	Unit
Beam energy	3.5	3.5	3.5	GeV
Natural emittance	31.8	33.36	26.3	pm-rad
Circumference	1080	810	810	m
Natural energy spread	$1.1 \times 10^{-3}$	$1.1 \times 10^{-3}$	$1.1 \times 10^{-3}$	
Length of LSS	5	6	6	m
RF frequency	166.6	166.6	166.6	MHz
RF voltage	1.9	2	2	MV
Corrected chromaticity (H/V)	+5/+5	+5/+5	+5/+5	
Momentum compaction factor	$1.37 \times 10^{-5}$	$2.52 \times 10^{-5}$	$3.61 \times 10^{-5}$	
Harmonic number	600	450	450	
Natural bunch length	4.6	5.1	5.8	mm
Betatron tune (H/V)	81.23/64.18	76.12/49.27	78.21/44.16	
Radiation energy loss per turn	0.898	0.904	0.768	MeV/turn
Damping partition [x/y/z]	1.55/1/1.45	1.5/1/1.5	1.63/1/1.37	
Damping time [x/y/z]	18.1/28.1/19.3	14/20.9/13.9	15.1/24.6/17.9	ms
$\beta$ function at LSS	3.4917/2.8481	4.87/4.55	5.11/2.74	m

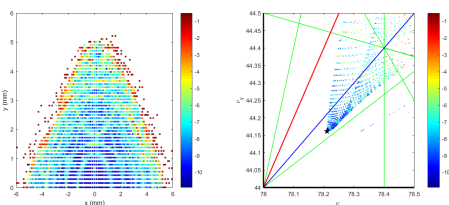


Figure 4: Dynamic aperture and frequency map analysis obtained after tracking over 1024 turns of Design III for SAPS (color bar represents stability of particles; blue and red imply more regular and chaotic motions, respectively).

Based on the new lattice and the evaluated impedance, the MWI threshold of Design III is calculated with ELEGANT with the bunch lengthened by a factor of 6 with harmonic cavities and the MWI threshold is about 420 mA. To suppress the IBS-induced emittance growth, the bunch is also lengthened by a factor of 6, and transverse coupling is 10% and 90% buckets are filled with bunches. The equilibrium emittance is obtained, which is about 52.2 pm-rad. With the above beam parameters, the Touschek lifetime is about 8.6 h. More details are seen in Ref. [16].

## CONCLUSION

With the increasingly clear parameter requirements, the SAPS lattice is continuously undergoing extensive design and optimization. In this paper, by combining three TLGB/RB unit cells with the hybrid-7BA lattice, and adding horizontally focusing quadrupoles inside the outer LGBs, a new lattice which basically meets the above requirements is obtained. However, a higher beam current is still pursued and more related optimization will be studied in the coming time, as well as other lattice options.

## ACKNOWLEDGMENTS

This work was supported by the Basic and Applied Basic Research Foundation of Guangdong Province (No. 2019B1515120069) and National Natural Science Foundation of China (No. 11922512 and No.12275284).

## REFERENCES

- [1] R. Hettel , “DLSR design and plans: an international overview”, *J. Synchrotron Radiat.*, vol. 21, 2014. doi:10.1107/S1600577514011515
- [2] M. Johansson *et al.*, “Magnet design for a low-emittance storage ring”, *J. Synchrotron Radiat.*, vol. 21, 2014. doi:10.1107/S160057751401666X
- [3] E. AlDmour *et al.*, “Diffraction-limited storage-ring vacuum technology”, *J. Synchrotron Radiat.*, vol. 21, 2014. doi:10.1107/S1600577514010480
- [4] M. M. Dehler *et al.*, “Conceptual Design for SLS-2”, in *Proc. FLS’18*, Shanghai, China, Mar. 2018, pp. 150–153. doi:10.18429/JACoW-FLS2018-WEP2PT038
- [5] S.C. Leemann *et al.*, “Perspectives for future light source lattices incorporating yet uncommon magnets”, *Phys. Rev. Spec. Top. Accel Beams*, vol. 14, p. 030701, 2011. doi:10.1103/PhysRevSTAB.14.030701
- [6] A. Streun , “The anti-bend cell for ultralow emittance storage ring lattices”, *Nucl. Instrum. Methods Phys. Res., Sec. A*, vol. 737, pp. 148-154, 2014. doi:10.1016/j.nima.2013.11.064
- [7] M. Borland *et al.*, “Lattice design challenges for fourth-generation storage-ring light sources”, *J. Synchrotron Radiat.*, vol. 21, 2014. doi:10.1107/S1600577514015203
- [8] P.F. Tavares *et al.*, “The MAX IV storage ring project”, *J. Synchrotron Radiat.*, vol. 21, pp. 862-877, 2014. doi:10.1107/S1600577514011503
- [9] L. Liu *et al.*, “The Sirius project”, *J. Synchrotron Radiat.*, vol. 21, 2014. doi:10.1107/S1600577514011928
- [10] L. Farvacque *et al.*, “A Low-Emittance Lattice for the ESRF”, in *Proc. IPAC’13*, Shanghai, China, May 2013, paper MO-PEA008, pp. 79–81.
- [11] M. Borland, “Simulation of Swap-Out Reliability for the Advance Photon Source Upgrade”, in *Proc. NAPAC’16*, Chicago, IL, USA, Oct. 2016, pp. 881–883. doi:10.18429/JACoW-NAPAC2016-WEPOB02
- [12] Y. Jiao *et al.*, “The HEPS project”, *J. Synchrotron Radiat.*, vol. 25, 2018. doi:10.1107/S1600577518012110

- [13] Z. H. Bai *et al.*, “A Modified Hybrid 6BA Lattice for the HALF Storage Ring”, in *Proc. IPAC’21*, Campinas, Brazil, May 2021, pp. 407–409.  
doi:10.18429/JACoW-IPAC2021-MOPAB112
- [14] Y. Zhao *et al.*, “Design study of APS-U-type hybrid-MBA lattice for mid-energy DLSR”, *Nucl. Sci. Tech.*, vol. 32, 71, 2021. doi:10.1007/s41365-021-00902-1
- [15] S. Wang *et al.*, “Proposal of the Southern Advanced Photon Source and Current Physics Design Study”, in *Proc. IPAC’21*, Campinas, Brazil, May 2021, pp. 300–303.  
doi:10.18429/JACoW-IPAC2021-MOPAB075
- [16] Y. Zhao *et al.*, “Improving the MWI threshold of the modified hybrid-7BA lattice design for SAPS”, submitted for publication.
- [17] J. Citadini *et al.*, “Sirius-Details of the New 3.2 T Permanent Magnet Superbend”, *IEEE Trans. Appl. Supercond.*, vol. 28, 3, 2017. doi:10.1109/TASC.2017.2786270
- [18] K.L. Brown and R.V. Serrvranckx, “First and second-order charged particle optics”, SLAC, SLAC-PUB-3381, July 1984.
- [19] I. V. Agapov *et al.*, “PETRA IV Storage Ring Design”, in *Proc. IPAC’22*, Bangkok, Thailand, Jun. 2022, pp. 1431–1434.  
doi:10.18429/JACoW-IPAC2022-TUPOMS014
- [20] J. Kim, X. Huang, P. Raimondi, J. A. Safranek, M. Song, and K. Tian, “A Hybrid Multi-Bend Achromat Lattice Design for SSRL-X”, in *Proc. IPAC’22*, Bangkok, Thailand, Jun. 2022, pp. 207–209.  
doi:10.18429/JACoW-IPAC2022-MOPOST054